한국기계가공학회지, 제17권, 제3호, pp.22～27(2018.06) ISSN 1598-6721(Print)
Journal of the Korean Society of Manufacturing Process Engineers, Vol. 17, No. 3, pp.22~27(2018.06) ISSN 2288-0771(Online)

https://doi.org/10.14775/ksmpe.2018.17.3.022

# Discrete Element Method using the Superposed Rigid-Rod Model for the Dynamic Behavior of Needle-Shaped Powder with a High Aspect Ratio

YoungHo Kim*, Junyoung Park**,#

*Remelt Eng. Team, Ulsan Aluminium Limit., **Dept. Mech. Dsgn. Eng., Kumoh Nat. Inst. Tech.

# 높은 세장비를 가진 침상형 입자의 동적 거동 해석을 위한 중첩형 강체막대모델을 이용한 이산요소법

김영호*, 박준영**,#

*(주)울산알루미늄 주조설비관리팀, **금오공과대학교 기계설계공학과

(Received 17 April 2018; received in revised form 25 April 2018; accepted 1 May 2018)

## ABSTRACT

One problem of the Discrete Element Method is the assumption of a spherical particle shape, which reduces the computing time but significantly limits the application of the DEM to analysis. This limitation can be overcome by a recently developed rigid-rod model. However, the rigid-rod model has an essential problem related with friction: it always contains friction error because of the bumpy surface. To overcome this issue, we suggest a superposed rigid-rod model in this paper. The superposed rigid-rod model is notably consistent with the theoretical value in terms of the velocity and angular velocity after the collision. The estimated error is negligible(less than 2%). Then, the developed model is applied to hopper discharging. The developed model shows no problem in the discharging flow from the hopper.

**Key Words :** Powder(분체), Needle-Shaped Particle(침상형 입자), Discrete Element Method(이산요소법)

## 1. Introduction

Generally, spherical particles are employed in processing where a large amount of particles are used. Sharp edged and slander particles can affect the surface of the workpiece excessively, which is why spherical particles are used. In recent years, much attention has been paid to magnetic polishing, in which polishing and magnetic particles are mixed and used. However, even in magnetic polishing, spherical particles are utilized[1-4]. Nonetheless, shot peening or shot blasting processing, in which surface hardness is more important or scale peeling is more influential than surface roughness, may use grit ,which has a slenderness ratio[5]. Naturally, surface roughness varies significantly depending on the use of spherical particles or grit.

# Corresponding Author : pcello@kumoh.ac.kr
Tel: +82-54-478-7377, Fax: +82-54-478-7377

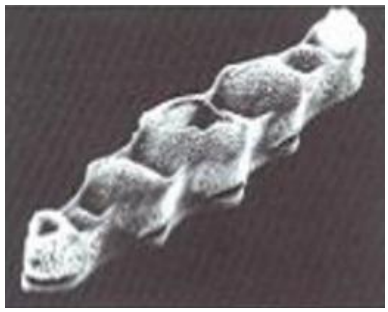

**Fig. 1 The shape of diatomite**

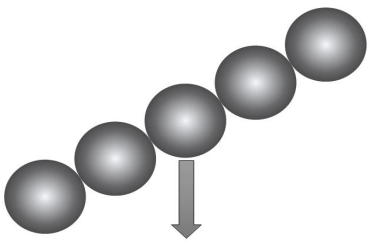

**Fig. 2 Rigid rod model**

The dynamic behavior of a large number of particles has been largely dealt with in powder technology. Even in the powder technology field, the shape of such particles has been known to be significantly influential on experiments. In particular, the fact that the shape can affect the particle fluidity significantly is well-known. Moreover, spherical particles are rarely present and the shapes of particles found in nature are generally considerably random[6].

However, most analyses are conducted assuming that the shapes of particles are all spherical because of the difficulties in analysis or calculation in practice[7]. This is directly related to the problem of defining the particle size, so it is applied to equivalent volume diameter or equivalent surface diameter etc. That is, it is expressed by a spherical diameter that has the same volume or surface area as the actual particle's volume or surface area.

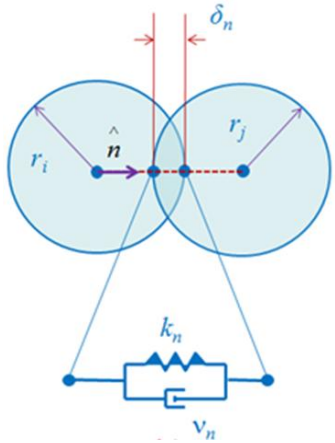


(a) Normal spring

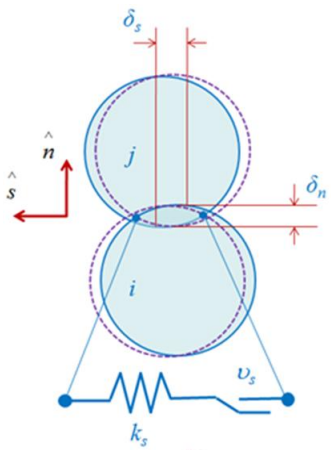


(b) Tangential spring

**Fig. 3 Particle-particle contact force**[10]

t

This assumption causes an inevitable error. For example, the fluid flows with spherical particles and fluid flows with slander particles, such as diatomite, as shown in Fig. 1, will have a significant difference in the viscosity coefficient.

The same problem is also found in the general discrete element method (DEM), which has been most widely used in numerical analysis on particle flow in particle technology. DEM usually assumes that all particles are spherical to simplify the calculation of the distance between particles[8].

To solve this, polyhedral elements have been

utilized, but the calculation time increases exponentially. Thus, some researchers have developed a rigid bar element where spherical particles are attached consecutively[9]. In addition, the two-dimensional model has been developed by the author[10]. However, a rigid bar element, as shown in Fig. 2, involves an excessive level of bumpiness on the particle surface, resulting in the problem of over emphasizing the friction between particles. Thus, this study developed a model that can minimize the effect of bumpy shape by the intended superposition between particles and verified the model. In addition, the model's compatibility was verified by applying the verified model to the hopper flow, like the previous study.

## 2. Discrete element method

### 2.1 General model

In general DEM, only gravitational force and contact force that occurred due to the motion of each of the particles are considered. The contact force is then divided into the normal force that acted in the normal direction of the collision and the tangential force that acted in the tangential direction. Generally, the collision of particles is regarded as the spring-mass system to calculate the contact force. The spring is shown in Fig. 3.

The acceleration and angular acceleration of each particle can be obtained by dividing the force and moment calculated by these springs using the mass and mass moment of each particle. After this, the speed, acceleration, position, and rotation amount can be calculated through numerical integration.

### 2.2 Rigid bar model

The general rigid bar model makes a slander shape connecting the number of particles by one row, as shown in Fig. 2. Thus, individual particles are restricted to relative motion so that both translational and rotational motions are not possible. That is, the location of each particle is determined by the location and angle of the bar in a relative manner. However, the force and moment applied to the bar are calculated based on the particle unit so that the total force and moment applied to the bar are calculated.

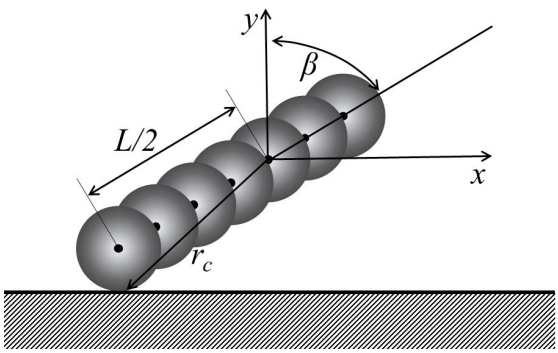


**Fig. 4 Schematics of superposed rigid rod model**

### 2.3 Superposed rigid rod model

A number of particles are arranged in a short distance, as shown in Fig. 4, to create a superposed rigid model. The same as the general rigid bar model, the relative motion of all particles is restricted and can be calculated only by the relative location in a bar. That is, the position of the particle is expressed relatively based on the bar's position. The contact force between superposed particles in a bar is ignored. Thus, the particle diameter in the superposed rigid bar model is expressed by two kinds in contrast with the general rigid bar model. That is, it can be divided into $d_r$, which represents the bar's diameter, and $d_{rf}$, which represents the particle's diameter except for particle superposition. Other physical properties are the same as those in the rigid bar model.

## 3. Model verification

To validate the model's effectiveness, the drop-and-bounce test was conducted, as shown in Fig.

5. A bar was shot to the floor at a constant speed without angular velocity with an initial angle, and then the bouncing speed and angular velocity from the floor were measured to compare them with the theoretical values. As shown in Fig. 5, the bar maintained the initial angle without any rotation until it collided with the floor, and the bouncing speed as well as angular velocity due to the collision were generated after collision.

The mass moment of inertia, which was essential to calculate the angular velocity, can be obtained as below, the same as in the previous rigid bar model[9,11].

$$I_{rod} = \sum_{n=1}^{n=N} [\frac{1}{10} + (n-1) - \frac{1}{2}(N-1)^2] M d_{rf}^2 \quad (1)$$

Here, $N$ refers to the number of particles in a single superposed rigid bar model, $M$ refers to the total mass of the superposed rigid bar model, and $d_{rf}$ refers to the diameter of the particle except for superposition.

The same as in the rigid bar model, the angular velocity in the rigid bar model after collision is expressed as below

$$\dot{\theta}_z^+ = \frac{M(\frac{L}{2} sin\beta)(1+\epsilon)}{I_{rod} + M(\frac{L}{2} sin\beta)^2} \cdot V_{y,CM}^- \quad (2)$$

Here, L is a length of the superposed rigid bar model $\beta$ is the initial angle, $\epsilon$ is the coefficient of restitution, and $V_{y,CM}^-$is the speed at the mass center in the superposed rigid bar model prior to collision. Similarly, the speed of the rigid bar model after collision is expressed by a function of the coefficient of restitution and angular velocity of the particle after collision in the following equation.

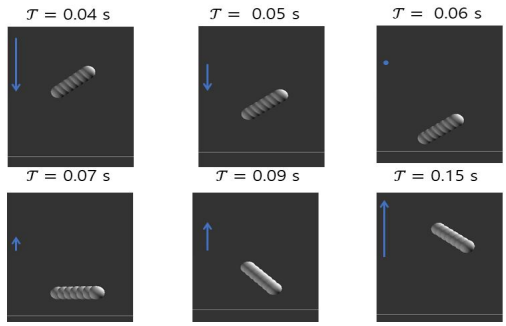


**Fig. 5 Snapshots for drop-and-bounce test**

**Table 1 Parameters used in the calculation**

| Parameter | Value |
|---|---|
| Mass of a particle, $m_p[kg]$ | 2.659e-04 |
| Number of particles, N | 7 |
| Diameter of particle, d[m] | 0.01 |
| Mass of fiber, $m_f[kg]$ | 1.861e-03 |
| Length of fiber, L [m] | 0.03 |
| Resitution coefficient, $\epsilon$ | 0.8 |
| Velocity before collision, $V_{y,CM}^+[m/s]$ | -2.0 |
| Normal spring stiffness, $K_n$ | $2.006\times10^{07}$ |
| Normal damping coefficient, $v_n$ | 15.807 |

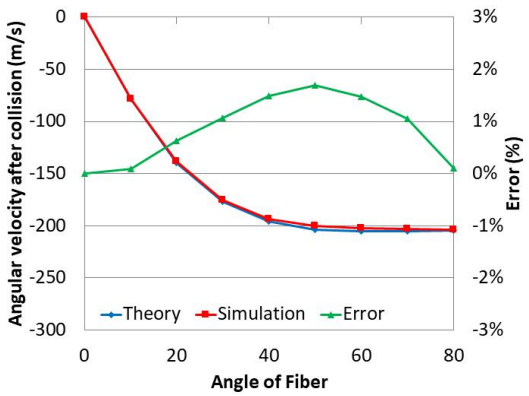


**Fig. 6 Angular velocity after collision**

$$V_{y,CM}^+ = -\epsilon V_{y,CM}^- + (\frac{L}{2} sin\beta)\dot{\theta}_z^+ \quad (3)$$

The parameter values used in the validation are presented in Table 1.

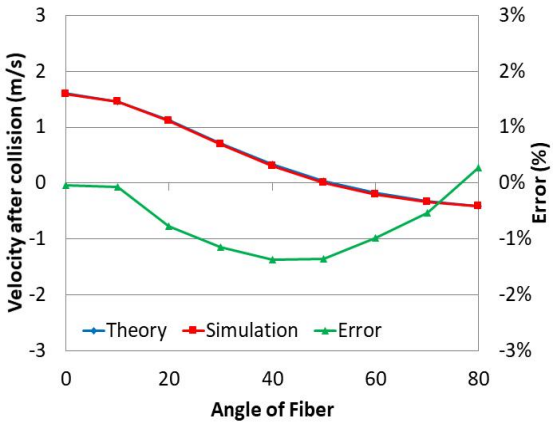


**Fig. 7 Velocity after collision**

Since the bar velocity of the mass center prior to collision is 2m/s, the bounding speed of the particle is theoretically 1.6 m/s. However, this bouncing velocity can differ depending on the initial angle. Thus, the bounicing velocity calculated by Eq. (3) and by DEM simulations are shown in Fig. 6. As shown at Fig. 6, the theoretical and simulation values were nearly the same and all measurement errors were within 1.5%, which indicated high accuracy.

The velocity after collision varies depending on the angular velocity after collision, as presented in Eq. (3). Thus, it is necessary to compare angular velocities before and after collision. In this paper, for angular velocities after collision, the theoretical value calculated via Eq. (2) and angular velocity measured through simulation are shown in Fig. 7. The angular velocity after collision also had an ignorable level of error within 2%, the same as shown in the velocity case above. The largest error was shown at around 50 degrees, and the smallest error was shown at around zero and 80 degrees.

## 4. Application of the developed model

Particles are used in many industrial processes, and a hopper or silo is a typical facility for storing

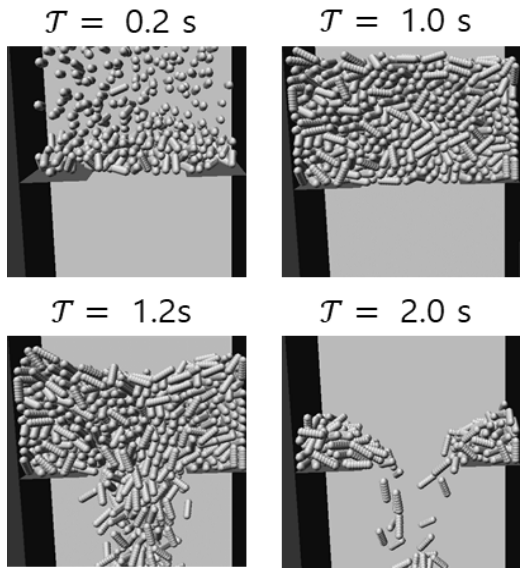


**Fig. 8 Snapshots for hopper discharging**

particles for a long or short period of time. Simulations were conducted to verify whether the superposed rigid bar model was effectively applied to discharging processes after storage.

Initially, the superposed bar was layered on the upper side of the hopper. The layering was performed for 1 sec and then discharged for 1 sec. As shown in Fig. 8, layering started at T=0.2 sec and was nearly finished at T=1.0 sec. Afterward, discharging started at T=1.2 sec so that a large number of superposed bars were discharged to the lower side through the outlet. At T=2.0 sec, most particles were already discharged, as shown in the figure. As expected, the superposed rigid bar model effectively simulated the flow of particles with a high slenderness ratio, the same as shown in the general rigid bar model.

## 5. Conclusion

To solve the problem related to the use of spherical particles, which has been pointed out as a limitation

of the general DEM, a rigid bar model has been widely used. However, the rigid bar model inevitably causes the bumpiness problem. Thus, this study proposed a superposed rigid bar model by allowing superposition and connecting a number of particles consecutively to overcome the bumpiness problem. The proposed model was verified through the drop-and-bounce test, and the test results verified that both the speed and angular velocity had a negligible level of errors within 2%. In addition, the developed model was applied to the hopper flow to verify the applicability of the model.

## Acknowledgment

This study was supported by a grant from the sabbatical/research year of the Kumoh National Institute of Technology.

## REFERENCES

1. Lee, Y. C., Shin, G. H., Kwak, T. S., “Deburring Technology of Vacuum Plate for MLCC Lamination Using Magnetic Abrasive Polishing and ELID Process,” Journal of the Korean Society of Manufacturing Process Engineers, Vol. 14, No. 3, pp. 149-154, 2015.
2. Lee, Y. C., Kim, K. S., Kwak, T. S., Lee, J. R., “An Experimental Study on Magnetic Assisted Polishing of Polycarbonate Plate for Recycling,” Journal of the Korean Society of Manufacturing Process Engineers, Vol. 12, No. 3, pp. 1-6, 2013.
3. Son, C. B., Ryu, M. H., Kwak, J. S., “Determination of Curvature Radius of Magnetic Tool Using Weighted Magnetic Flux Density in Magnetic Abrasive Polishing,” Journal of the Korean Society of Manufacturing Process Engineers, Vol. 12, No. 3, pp. 69-75, 2013.
4. Kwak, T. S., Kwak, J. S., “Magnetic Abrasive Polishing Technology with Ceramic Particles,” Journal of the Korean Society for Precision Engineering, Vol. 30, No. 12, pp. 1253-1258, 2013.
5. Chung, S. K., Introductory for Shot Peening Process, Sehwa Publication, pp.123-160, 2001.
6. Kang, S. H., Lyu, P.J., Park, J., Choi, H. K., Powder Process Engineering, pp.1-20, 2012.
7. Choi, D. M., Park, J., “Discrete element method for predicting the coverage at shot peening processing,” Fall Conference of the Korean Society of Manufacturing Process Engineers, Vol. 1, pp. 41-41, 2014.
8. Cundall, P. A., Strack, O. D. L., “A discrete numerical model for granular assemblies,” Geotechnique, Vol. 29, No. 1, pp. 47-65, 1979.
9. Ahn, S. h., Park, J., “A New Rigid Rod Model for the Discrete Element Method to Analyze the Dynamic Behavior of Needle-shaped Powder,” Journal of the Korean Society of Manufacturing Process Engineers, Vol. 16, No. 2, pp. 149-154, 2017.
10. Park, J., "Modelling the Dynamics of Fabric in a Horizontal Drum," Doctoral disssertation, Purdue University, U.S., 2003.
11. Park, J., Kang, N., “Applications of fiber models based on discrete element method to string vibration,” Journal of Mechanical Science and Technology, Vol. 23, pp. 372-380, 2009.